release of 23 residues that causes the loss of polymerization.

ACKNOWLEDGMENTS

I thank Dr. Manuel F. Morales for invaluable discussions and comments during the course of this work and for many helpful suggestions in the preparation of the manuscript. I am grateful to Dr. Reiji Takashi for valuable discussions and for donating Gln-44-labeled actin.

Registry No. ATPase, 9000-83-3.

REFERENCES

Burtnick, L. D. (1984) *Biochim. Biophys. Acta 791*, 57–62.
Chantler, P. D., & Gratzer, W. B. (1975) *Eur. J. Biochem. 60*, 67–72.
Duke, J., Takashi, R., Ue, K., & Morales, M. F. (1976) *Proc. Natl. Acad. Sci. U.S.A. 73*, 302–306.
Elzinga, M., Collins, J. H., Huehl, W. M., & Adelstein, R. S. (1973) *Proc. Natl. Acad. Sci. U.S.A. 70*, 2687–2691.
Jacobson, G., & Rosenbusch, J. P. (1976) *Proc. Natl. Acad. Sci. U.S.A. 73*, 2742–2746.
Johnson, P., Wester, P. J., & Hidaka, R. S. (1979) *Biochim. Biophys. Acta 578*, 253–257.
Konno, K. (1987) *J. Biochem. (Tokyo)* (submitted for publication).
Konno, K., & Morales, M. F. (1985a) *Biophys. J. 47*, 218a.
Konno, K., & Morales, M. F. (1985b) *Proc. Natl. Acad. Sci. U.S.A. 82*, 7904–7908.
Laemmli, U. K. (1970) *Nature (London) 277*, 680–685.
Lazarides, E., & Lindberg, U. (1974) *Proc. Natl. Acad. Sci. U.S.A. 71*, 4742–4746.
Mornet, D., & Ue, K. (1984) *Proc. Natl. Acad. Sci. U.S.A.* 81, 3680–3684.
Mornet, D., & Ue, K. (1985) *Biochemistry 24*, 840–846.
Mornet, D., Bertrand, R., Pantel, P., Andemard, E., & Kassab, R. (1981) *Biochemistry 20*, 2110–2120.
Mornet, D., Ue, K., & Morales, M. F. (1984) *Proc. Natl. Acad. Sci. U.S.A. 81*, 736–739.
Rich, S. A., & Estes, J. E. (1976) *J. Mol. Biol. 104*, 777–792.
Spudich, J. A., & Watt, S. (1971) *J. Biol. Chem. 246*, 4866–4871.
Sutoh, K. (1982) *Biochemistry 21*, 3654–3661.
Sutoh, K. (1983) *Biochemistry 22*, 1570–1585.
Takashi, R., & Kasprzak, A. (1985) *Biophys. J. 47*, 26a.
Weeds, A. G., & Taylor, R. S. (1977) *Nature (London) 257*, 54–56.
Weiner, A. M., Plott, T., & Weber, K. (1972) *J. Biol. Chem. 247*, 3242–3251.
Yamamoto, K., & Sekine, T. (1979) *J. Biochem. (Tokyo) 86*, 1855–1862.

Cross-Linking within the Thick Filaments of Muscle and Its Effect on Contractile Force†

Hitoshi Ueno and William F. Harrington*
Department of Biology, McCollum-Pratt Institute, The Johns Hopkins University, Baltimore, Maryland 21218
Received October 20, 1986; Revised Manuscript Received February 18, 1987

ABSTRACT: We have examined the effect of cross-linking on cross-bridge movement and isometric force in glycerinated *psoas* fibers. Two different methods, high-porosity gel electrophoresis and a fractionation technique, were used to follow the cross-linking of myosin heads (subfragment 1) and rod segments to the thick filament backbone. Contrary to earlier reports [Sutoh, K., & Harrington, W. F. (1977) *Biochemistry 16*, 2441–2449; Sutoh, K., Chiao, Y. C., & Harrington, W. F. (1978) *Biochemistry 17*, 1234–1239; Chiao, Y. C., & Harrington, W. F. (1979) *Biochemistry 18*, 959–963], we find that the heads of the myosin molecules are not cross-linked to the thick filament surface by dimethyl suberimidate. The time dependence of cross-linking rod segments within the core was monitored by a disulfide oxidation procedure to distinguish between intermolecular and intramolecular cross-linking. Comparison of the extent of the cross-linking reaction within myofibrils and the isometric force developed within fibers at various stages of cross-linking shows that isometric force is abolished in parallel with the formation of high molecular weight (cross-linked) rod species ($\geq M_r$ 1000K). The myofibrillar ATPase remains virtually unaffected by the cross-linking reaction.

Baker and Cooke (1986) have recently reported that on cross-linking of glycerinated psoas fibers with dimethyl suberimidate (DMS),[1] ATP hydrolysis, force generation, and shortening can still occur after the S-2 region of myosin has been cross-linked to the thick filament core. On the basis of these findings, they suggest that models of muscle contraction [e.g., see Harrington (1971, 1979)] which involve large-scale shortening of S-2 during a cross-bridge cycle can be excluded. In the studies of Baker and Cooke, cross-linking of the S-2 segment was inferred from the time-dependent decay kinetics of the S-1 band following gel electrophoresis of the proteolytically digested cross-linked products. This interpretation is based on earlier studies in our own laboratory (Sutoh & Harrington, 1977; Sutoh et al., 1978; Chiao & Harrington,

† This work was supported by NIH Grant AM 04349 (to W.F.H.). Contribution No. 1366 from the Department of Biology, McCollum-Pratt Institute, The Johns Hopkins University.

[1] Abbreviations: MHC, rabbit skeletal myosin heavy chain; HMM, heavy meromyosin; LMM, light meromyosin; S-1, subfragment 1; S-2, subfragment 2; Rod^{S}_{S}, LMM^{S}_{S}, and $S\text{-}2^{S}_{S}$, rod, LMM, and S-2, respectively, with interchain disulfide bond(s); MHC^{SH}_{SH}, HMM^{SH}_{SH}, and LMM^{SH}_{SH}, myosin heavy chain or its subfragments without an interchain disulfide bond; TM, tropomyosin; TM^{S}_{S}, tropomyosin with an interchain disulfide bond; DMS, dimethyl suberimidate; DTBP, dimethyl 3,3′-dithiobis(propionimidate); SDS, sodium dodecyl sulfate; EDTA, ethylenediaminetetraacetic acid; Tris, tris(hydroxymethyl)aminomethane; PC_r, phosphocreatine; DTT, dithiothreitol; kDa, kilodalton(s); EGTA, ethylene glycol bis(β-aminoethyl ether)-*N*,*N*,*N*′,*N*′-tetraacetic acid.

0006-2960/87/0426-3589$01.50/0

1979) in which we proposed that the heads of the myosin molecules are covalently bound to the thick filament surface under similar cross-linking conditions at neutral pH. We now have reason to suspect this interpretation on the basis of the following: (1) To date, there has been no direct evidence to demonstrate that S-1 is cross-linked to neighboring rod segments in the filament core. Rather, such intramolecular cross-linking was *deduced* from the disappearance of the S-1 band from its characteristic position on SDS gels following electrophoresis of the cross-linked products. (2) The time-dependent decrease in intensity of the S-1 band on SDS gels during cross-linking could result from formation of intramolecular cross-links of the S-1 subunit with its own light chain(s), thus forming higher molecular weight (~120K) species as suggested by Labbé et al. (1982). (3) In retrospect, the relative cross-linking rate between S-1 and rod (k_{S-1}/k_{rod} = 0.3 at neutral pH) seems unreasonably large when the contact surface area between S-1 and the thick filament backbone is compared to that of the rod segment and its neighbors in the core. (4) At alkaline pH, addition of divalent metal suppresses chymotryptic cleavage within the HMM/LMM hinge region of the rigor myofibrils (Borejdo & Weber, 1982; Ueno & Harrington, 1986) and rod filaments (Ueno et al., 1983). Under these conditions, the S-2 segment binds to the thick filament surface as directly revealed by cross-linking studies (Reisler et al., 1983). Nevertheless, we find (unpublished results) that the cross-linking rate of S-1 is virtually unaffected by divalent metal ions at alkaline pH.

In view of the conclusion of Baker and Cooke (1986) and its significance in understanding the origin of contractile force in muscle, we have reinvestigated the cross-linking process, paying particular attention to the disposition of the S-1 subunits. The effect of intermolecular cross-linking of rod segments in the thick filament core on the ATP cleavage reaction as well as the isometric force was also examined.

Materials and Methods

Myofibrils. Myofibrils were isolated according to the procedure of Kundrat and Pepe (1971) from glycerinated rabbit psoas muscle bundles prepared according to the procedure of Rome (1967). The approximate concentration of myofibrils was determined by dissolving them in 5% (w/v) SDS and measuring the absorbance assuming $E^{1\%}_{280nm}$ = 7.0 (Sutoh & Harrington, 1977). Myofibrils were equilibrated by repeated cycles of resuspension and centrifugation in the desired solvent.

Preparation of Single Fibers. Single fibers or bundles of two to three fibers were dissected from psoas fiber bundles which had been stored at −20 °C over periods of 1–3 weeks in 1:1 (v/v) glycerol-skinning solution (Brenner, 1983). Bundles were transferred to skinning solution for ~30 min at 0 °C prior to dissection. Skinned fiber segments 4–6 mm in length were glued to aluminum T clips which were provided with holes for mounting on the force transducer. The "T's" of the clips were folded across the ends of the fibers to increase bonding strength.

Cross-Linking of Myofibrils. Myofibrils (1–2 mg/mL) equilibrated with buffered solution (pH 7.2, $\mu \simeq 0.1$ M; see figure legends for more details) were cross-linked by dimethyl suberimidate (DMS) or dimethyl 3,3′-dithiobis(propionimidate) (DTBP). DMS and DTBP were purchased from Pierce Chemical Co. (Rockford, IL). The cross-linking reaction was stopped at various times by adding an equal volume of 0.10 M ethanolamine in 40 mM cacodylate (pH 7.0) followed by centrifugation of the mixture. The pellet was homogenized with 40 mM cacodylate and 80 mM NaCl, pH 7.2 (solvent A). This centrifugation and homogenization cycle was repeated in solvent A.

Cross-Linking of a Single Fiber. Glycerinated rabbit psoas fibers were cross-linked with DMS (2.0 mg/mL) in 40 mM cacodylate and 80 mM NaCl (pH 7.2) at 10 °C. The cross-linking reaction was quenched at various times by washing the fibers in 0.1 M ethanolamine/40 mM imidazole hydrochloride (pH 7.0). The time course of cross-linking was examined by dissolving the fiber (~5 mm in length) in 20 μL of SDS-containing solution [1% (w/v) SDS, 0.125 M Tris·HCl, pH 6.8, 10% (v/v) glycerol, 0.1% (v/v) 2-mercaptoethanol, and a trace of bromophenol blue]. Protein samples were boiled for 1 min. Following electrophoresis of the sample (10 μL) on SDS-containing minislab gels, the myosin heavy chain band (MHC^{SH}_{SH}) intensity (normalized to the actin band intensity) was determined. The normalized MHC^{SH}_{SH} intensity decays in time as a first-order process (2.4 h^{-1}, 22 samples examined).

Oxidation and Proteolytic Digestion of Myofibrils. Myofibrils which had been cross-linked with DMS for various periods of time were oxidized prior to digestion to introduce disulfide links within individual rod segments (Ueno & Harrington, 1981). Myofibrils (~2 mg/mL in solvent A) were mixed with an equal volume (0.50 mL) of 20 μM $CuCl_2$ in solvent A and left at room temperature for 20–30 min. During this period, oxidized forms of myosin rod (Rod^{S}_{S}) as well as tropomyosin (TM^{S}_{S}) are observed (e.g., Figure 1B). Oxidation was terminated by adding 1 mL of 40 mM imidazole hydrochloride, 80 mM NaCl, and 5 mM EDTA (solvent B), followed by centrifugation. The pellet was rehomogenized in solvent B (final volume ≃ 0.7 mL), and 40 mL of α-chymotrypsin (1.0 mg/mL dissolved in 1 mM HCl) was added to the myofibril suspension (0.7 mL) to digest the S-1/rod junction at 23 °C for 25 min. Digestion was quenched by adding 25 μL of phenylmethanesulfonyl fluoride [1% (w/v) dissolved in ethanol]. The reaction mixture was finally mixed with 1 mM iodoacetamide and 10% SDS (0.1 mL), immediately boiled for 2 min, and then exhaustively dialyzed against 10% glycerol, 0.1% SDS, 50 mM Tris·HCl (pH 6.8), and a trace of bromophenol blue. To obtain the reduced form of rod (Rod^{SH}_{SH}), the dialysate was mixed with 0.1 volume of 5% 2-mercaptoethanol and 0.3 M Tris·HCl (pH 8.8) and left overnight.

The effect of chemical cross-linking of myofibrils on the chymotryptic cleavage rates at the head/rod junction was examined. Myofibrils were cross-linked with DMS, and the reaction was quenched by ethanolamine at various stages of cross-linking. Cross-linked myofibrils were digested by chymotrypsin in the presence of EDTA to cleave the rod/S-1 junction and the kinetics of cleavage compared following SDS gel electrophoretic analyses of the digests. Half-times of the cleavage were about 2 min under the present digestion conditions, irrespective of the stage of DMS cross-linking of myofibrils. This indicates that the chemical cross-linking of myofibrils has very little effect on the chymotryptic cleavage at the S-1/rod junction.

Sodium Dodecyl Sulfate Containing Polyacrylamide Gel Electrophoresis. SDS–polyacrylamide gel electrophoresis was carried out according to the method of Laemmli (1970) employing a minislab gel apparatus (10 cm × 8 cm × 0.8 mm; Idea Scientific, Corvallis, OR). Acrylamide/methylenebis(acrylamide) was 30:0.80 (w/w). (Gel concentrations are given as percent acrylamide in the text.) Peptide bands were stained with Coomassie Brilliant Blue G-250. Peptide band intensities were determined on a gel scanning densitometer

(LKB 2202 and 2220, Bromma, Sweden).

Sodium Dodecyl Sulfate Containing Agarose–Polyacrylamide Gel Electrophoresis. Agarose (0.5%)–polyacrylamide (2.5%) gels (Peacock & Dingman, 1968) were prepared according to Rodgers (1982); 80 mL of gel solution was prepared as follows: a mixture of 29 mL of stock buffer [0.2 M sodium phosphate buffer/0.2% SDS (pH 7.0)], 22 mL of water, and 0.4 g of agarose was heated at 80 °C for 15 min and then cooled to 55 °C. This mixture was added to a second solvent (at 55 °C) containing 11 mL of stock buffer, 8.9 mL of acrylamide (21.4%)/bis(acrylamide) (1.1%) solution, 2.1 mL of water, and 5 mL of 6.4% 3-(dimethylamino)propionitrile. Finally, 2 mL of 1.6% ammonium persulfate was added to the whole mixture, which was then poured onto slab gel plates (12 cm × 12 cm × 1.5 mm). Gel buffer was 0.1% SDS and 0.1 M sodium phosphate buffer (pH 7.0).

Two-Dimensional Gel Electrophoresis. Two-dimensional gels were occasionally used to identify the protein bands unambiguously. Myofibrils cross-linked with DTBP were oxidized by cupric ions, followed by α-chymotryptic digestion. After denaturing in SDS-containing solution, samples were run on agarose–polyacrylamide gels as described above for the one-dimensional gels. Gels were then sliced and soaked in 20 mM dithiothreitol, 0.5% 2-mercaptoethanol, 0.2% SDS, and 0.3 M Tris·HCl (pH 8.8) for 15–30 min at room temperature. These reduced gels were applied to 8% gels for the second dimension, employing a gel running buffer (50 mM Tris and 380 mM glycine, pH 8.3).

Myofibrillar ATPase. Myofibrils (2 mg/mL in 40 mM cacodylate and 80 mM NaCl, pH 7.2) at various stages of cross-linking were mixed with ATP solution (4 volumes), and the time course of inorganic phosphate release was measured according to Piper and Lovell (1981). ATP solution was 5 mM ATP, 10 mM $MgCl_2$, 60 mM NaCl, and 40 mM imidazole hydrochloride (pH 7.2) for actin-activated MgATPase measurements. For CaATPase measurements, 10 mM $MgCl_2$ was replaced by 10 mM $CaCl_2$.

Isometric Force Measurements. Glycerinated single or double fibers (see above) were mounted on a force transducer (404; Cambridge Technology, Cambridge, MA) and immersed in skinning solution in a small rectangular cell (5 × 2 × 1.5 mm) equipped with glass windows and a stainless-steel base which was fastened to a flow-through copper jacket for thermal equilibration. Temperature within the cell was maintained at 10 ± 1 °C throughout each experiment by circulating water from a temperature-regulated bath. The sarcomere length within the fiber was adjusted to 2.5 μm by using the diffraction pattern from a helium–neon laser. Following several changes of relaxing buffer (40 mM cacodylate, 5.6 mM $MgCl_2$, 2 mM ATP, 5 mM PCr, 2 mM EDTA, and 120 mM NaCl, pH 7.3), the fiber was activated (relaxing buffer + 2 mM $CaCl_2$) to obtain a "zero-time" force (f_0). After the fiber was relaxed, it was washed several times with rigor solution (40 mM cacodylate and 80 mM NaCl, pH 7.2, or 40 mM cacodylate, 20 mM $MgCl_2$, and 20 mM NaCl, pH 7.2) and then immersed in cross-linking solution. Each fiber was cross-linked for a given period of time, the reaction was quenched [0.1 M ethanolamine/40 mM imidazole hydrochloride (pH 7.0)], and following several changes of relaxing buffer, the fiber was again activated to obtain the relative isometric force (f/f_0).

Results

Kinetics of Cross-Linking S-1 Subunits in Myofibrils. Myofibrils were cross-linked with DMS at pH 7.2 and μ = 0.1 M. At various stages of cross-linking, aliquots were quenched and centrifuged to remove excess reagent, and the resulting myofibrillar pellet was dispersed and digested with α-chymotrypsin in the presence of EDTA to cleave the S-1/rod junction [e.g., see Weeds and Pope (1977)]. Since the aim of the present study was to clarify the process of cross-linking between the rod segments of the thick filament, myofibrils were oxidized prior to digestion to introduce disulfide links within individual rod segments (Ueno & Harrington, 1981). This procedure allows us to distinguish between cross-linking of individual heavy chains and the intermolecular cross-linking of the intact (two-chain) rod to form higher molecular weight rod species within the thick filament core. The extent of cross-linking S-1 and rod segments of myosin was determined by densitometry of the bands corresponding to those species following electrophoresis on SDS-containing gels as described under Materials and Methods.

Figure 1A shows SDS gels of myofibrils at various stages of cross-linking with DMS. In this experiment, all protein samples were treated with 0.5% 2-mercaptoethanol to reduce disulfide bonds prior to gel electrophoresis. The 125K band formed under these conditions is well documented and corresponds to the heavy chain of the rod segment of myosin. Chymotryptic digestion of the oxidized rod segment (Rod_S^S) produced an extra clip at M_r 10K from the S-1/rod junction to yield the M_r 115K band [see Reisler et al. (1983)]. The M_r 90K band corresponds to the intact heavy chain of the S-1 subunit. With increasing cross-linking time, peptide bands between the 90K and 125K bands are observed. The optical density of the 90K band (normalized to the actin band) decreased with time as reported earlier [e.g., see Sutoh and Harrington (1977)].

Since the polyacrylamide gel pattern is complicated by the presence of multiple, closely spaced migrating species, high-porosity gels were employed to resolve the pattern in electrophoresis runs of the oxidized myofibrillar system. Agarose (0.5%)–polyacrylamide (2.5%)–SDS gels of DMS cross-linked myofibrils *in the absence* of 2-mercaptoethanol are presented in Figure 1B. Oxidized myofibrils showed five major bands: M_r 260K oxidized rod (Rod_S^S), M_r 90K (S-1), M_r 70K oxidized tropomyosin (TM_S^S), M_r 43K actin, and M_r 27K band (a mixture of peptides). Each band of the pattern was identified in a separate experiment using DTBP as cross-linker and two-dimensional gel electrophoresis (see Materials and Methods); i.e., a gel of oxidized myofibrils was sliced and run on a second gel after reducing disulfide bonds. According to this procedure, the 27K band (see Figure 1B) was split into two more rapidly migrating peptide bands, suggesting that this species likely originates from disulfide cross-linking of two myosin light chains (and/or troponin subunits) which were partially clipped by chymotryptic digestion. On the basis of this procedure, the 90K and 120K bands on agarose–polyacrylamide gels (e.g., Figure 1B) were found to contain S-1 heavy chain (90K). It will be noted, as is also shown below, that the total intensity of the bands derived from the S-1 heavy chain remains essentially unchanged with cross-linking time. High molecular weight species corresponding to 500K, 750K, 1000K, and 1200K bands are seen near the tops of the gels (Figure 1B). These are formed through intermolecular cross-linking of intact (two-chain) myosin rods corresponding to $(Rod_S^S)_i$ where i = 2, 3, 4, and 5, respectively.

We also employed two-dimensional polyacrylamide–SDS gel electrophoresis to determine whether S-1 is cross-linked to the rod segment of myosin (data not shown). Myofibrils were cross-linked with DTBP (cleavable disulfide cross-linker), and the reaction was quenched by ethanolamine, as described under Materials and Methods. The cross-linked myofibrils

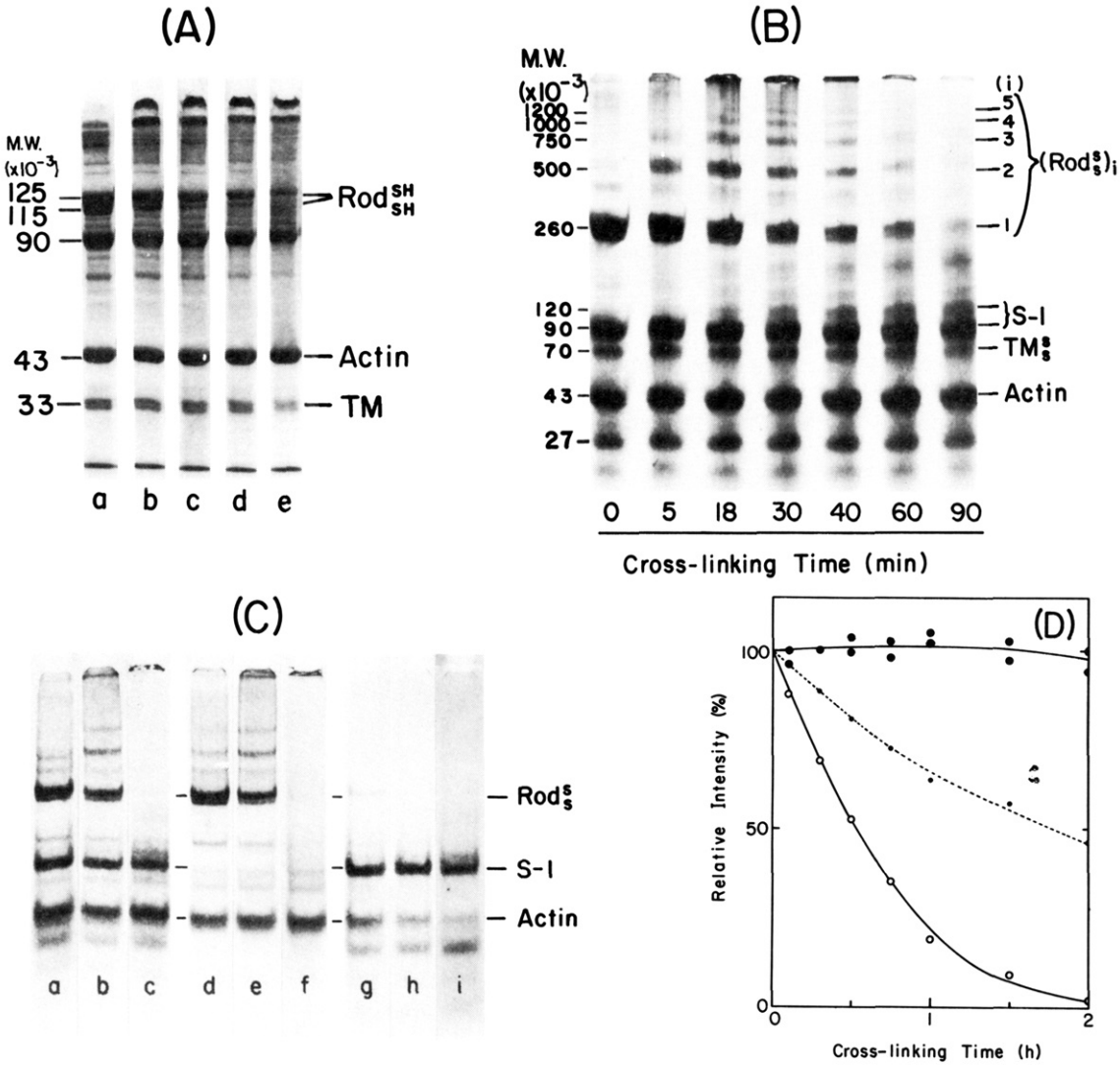

FIGURE 1: Chemical cross-linking of rabbit myofibrils with dimethyl suberimidate. Myofibrils (2 mg of protein/mL) were cross-linked by dimethyl suberimidate (1.0 mg/mL) in 40 mM imidazole hydrochloride and 80 mM NaCl (pH 7.2) at 22 °C. The S-1/rod junction in each sample was digested by chymotrypsin (see Materials and Methods), and the time course of cross-linking was analyzed by SDS gel electrophoresis. Prior to denaturation of samples, they were oxidized by cupric ions to introduce intramolecular interchain disulfide bond(s) into rod (Rod_S^S) as well as tropomyosin (TM_S^S). (A) Cross-linked myofibrils were run on SDS gels employing 5% and 8% stacking gels according to Laemmli (1970). Protein samples were fully reduced with 2-mercaptoethanol (10 mM). Cross-linking times (in minutes): (a) 0; (b) 3; (c) 20; (d) 35; (e) 60. (B) Cross-linked myofibrils were run on SDS-containing agarose (0.5%)–polyacrylamide (2.5%) gels. (C) Cross-linked myofibrils were oxidized by cupric ions and equilibrated in 40 mM imidazole hydrochloride, 80 mM NaCl, and 5 mM $MgCl_2$ (pH 7.2) by repeated centrifugation and homogenization. The samples were then mixed at 0 °C with 0.5 volume of 25 mM phosphocreatine, 10 mM $MgCl_2$, 8 mM ATP, and 70 mM NaCl (pH 7.3) followed by centrifugation (7000 rpm for 10 min). The precipitates (d–f) and supernatants (g–i) as well as the mixture (a–c) were run on SDS-containing agarose (0.5%)–polyacrylamide (2.5%) gels. Cross-linking times (in minutes): (a, d, g) 0; (b, e, h) 30; and (c, f, i) 120. (D) Relative band intensities of (○) rod (M_r 260K Rod_S^S) and (●) S-1 (M_r 90K + 120K) are plotted vs. cross-linking time (see Figure 1B). The dotted line shows the intensity of the M_r 90K S-1 band vs. cross-linking time shown in Figure 1A.

were oxidized by cupric ions to introduce disulfide bonds into the rod segments of myosin, followed by digestion with chymotrypsin to clip the S-1/rod linkage in the presence of EDTA. Electrophoresis of total digests on SDS-containing agarose (0.5%)–acrylamide (2.5%) gels gave patterns similar to Figure 1B, where DMS was used instead of DTBP. At times where ~20% and ~80% of the rods (Rod_s^s) were cross-linked, the peptide species were resolved by electrophoresis on agarose–acrylamide gels, and the resulting patterns (260K and higher species) were excised from the gels without prior staining of the peptide bands. All of the disulfide cross-links present (DTBP as well as intrinsic protein disulfide bonds) were then reduced by DTT and 2-mercaptoethanol (see Materials and Methods), and the status of the peptides in the reduced gels was examined by electrophoresis in a second gel (8% SDS-containing gel). Following staining, the resulting band pattern showed no migrating species corresponding to the S-1 heavy chain. This result demonstrates that S-1 is not cross-linked to rod or its higher order species $(Rod_S^S)_i$ under the present experimental conditions.

To provide further evidence that S-1 is not cross-linked to rod, myofibrils at various stages of cross-linking by DMS were digested with chymotrypsin in the presence of EDTA to cleave the S-1/rod junction. The digests were centrifuged in the presence of MgATP (pH 7, μ = 0.1 M) to dissociate S-1 from actin, and the supernatant and pellet fractions as well as the whole mixture were examined by electrophoresis on SDS-containing agarose–polyacrylamide gels. The rod segment and actin were recovered in the pellet, while the S-1 subunit was found exclusively in the supernatant (Figure 1C).

Figure 1D, which summarizes the present findings on the cross-linking of S-1 subunits in myofibrils, shows a plot of relative intensities of rod and S-1 segments (normalized to actin band intensities) vs. cross-linking time. The M_r 260K

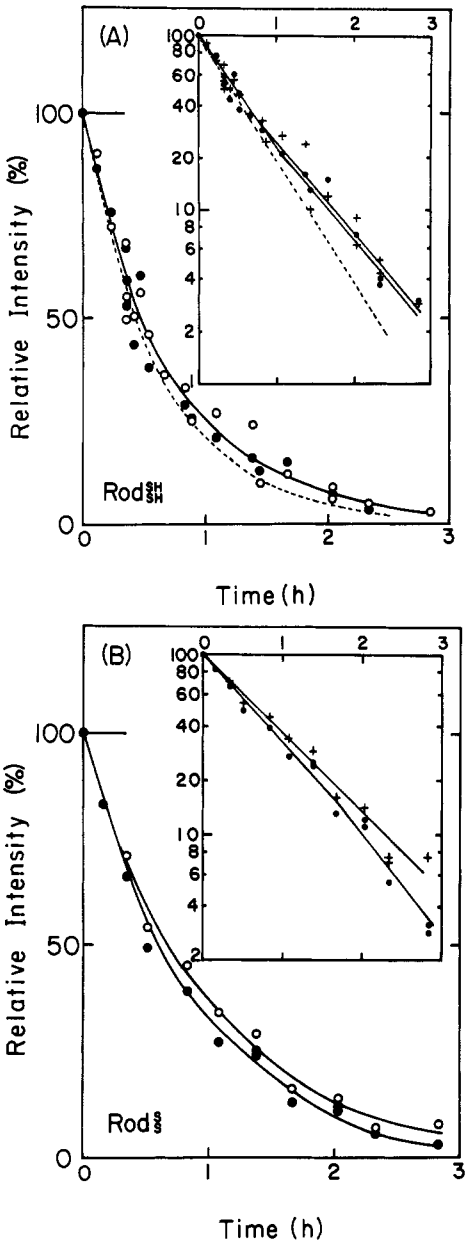

FIGURE 2: Time course of cross-linking of myofibrils. Myofibrils (1.2 mg of protein/mL) were cross-linked by dimethyl suberimidate (3 mg/mL) at 4 °C in 40 mM cacodylate and 80 mM NaCl, pH 7.2 (open circles and crosses), or in 40 mM cacodylate, 20 mM NaCl, and 20 mM $MgCl_2$, pH 7.2 (closed circles). The S-1/rod junction in each sample was digested by chymotrypsin before electrophoresis. Relative intensities of (A) reduced rod band (Rod^{SH}_{SH}), M_r 125K + 115K) and (B) oxidized rod band (Rod^{S}_{S}, M_r 260K) are plotted vs. cross-linking time. The legend to Figure A,B describes the experimental conditions of gel electrophoresis for (A) and (B) in this figure, respectively. Insertions are semilogarithmic plots of the same data. Three different sets of experiments are combined. Dotted lines are relative intensities of myosin heavy chain (MHC^{SH}_{SH}) vs. time plots (data points are not included).

rod band (Rod^{S}_{S}, open circles) obtained from Figure 1B followed a pseudo-first-order decay process, whereas the bands corresponding to the S-1 subunit (the 90- plus 120-kDa species; Figure 1B) were virtually invariant with time (closed circles). A plot of the intensity vs. time of the 90K species band (dotted line) obtained from densitometry of the gel in Figure 1A exhibits the characteristic time-dependent decay observed in earlier studies [e.g., see Sutoh and Harrington (1977)] using the polyacrylamide–SDS gel system. We conclude from the results described above that the S-1 subunits are not significantly cross-linked to rod segments of neighboring myosin

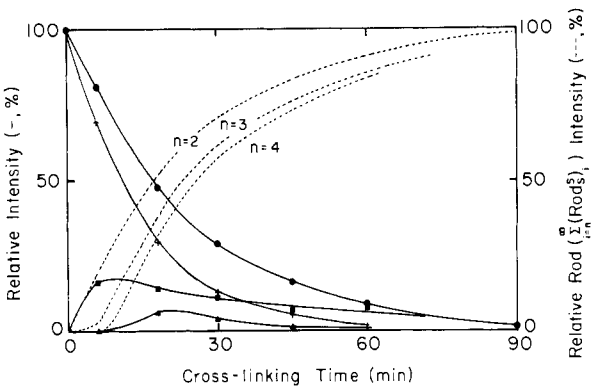

FIGURE 3: Time course of cross-linking reactions of myofibrils. Myofibrils cross-linked by dimethyl suberimidate as shown in Figure 1B are further analyzed. (+) MHC^{SH}_{SH}; (●) M_r 260K (Rod^{S}_{S}); (■) M_r 500K rod [$(Rod^{S}_{S})_2$]; (▲) M_r 750K rod [$(Rod^{S}_{S})_3$]. Dotted lines show the time course of increase in intermolecularly cross-linked rod species, $\sum_{i=n}^{\infty}(Rod^{S}_{S})_i$.

molecules within the thick filament core by either DMS or DTBP.

Kinetics of Cross-Linking Rod Segments in Myofibrils. (A) Comparison of Reduced (Rod^{SH}_{SH}) and Oxidized (Rod^{S}_{S}) Rod Subfragments after Cross-Linking with DMS. A major goal in the present study was to investigate the effects of chemical cross-linking within the myosin filament backbone on contractile force. To clarify the kinetics of formation of cross-links between individual rods, myofibrils were cross-linked with DMS, and the time course of intramolecular and intermolecular cross-linking was obtained by comparing gel patterns in their oxidized and reduced states as described under Materials and Methods and in the previous section. The time course of cross-linking rod segments (Figure 2) shows that cross-linking occurs in both the reduced rod (Rod^{SH}_{SH}) and the oxidized rod (Rod^{S}_{S}) in an approximately first-order reaction (see inserts to Figure 2). Figure 2A also presents the time course of cross-linking the myosin heavy chain (MHC^{SH}_{SH}). The rate constant for this cross-linking reaction is slightly larger than the rate constant observed for cross-linking the rod segment, probably as a result of uncertainty in identifying the bands corresponding to the rod segment, particularly at the later stages of the reaction.

(B) Effect of Divalent Metal. It has been shown in earlier studies that millimolar concentrations of divalent metal ion promote association of the S-2 segment of the rod with the filament backbone (Ueno et al., 1983; Ueno & Harrington, 1986; Reisler et al., 1983; Persechini & Rowe, 1984). We have therefore compared the cross-linking rates of the rod in the presence and absence of Mg^{2+}. The cross-linking rate constant of Rod^{S}_{S} was 15% lower than that of Rod^{SH}_{SH} in the absence of Mg^{2+}. In the presence of 20 mM Mg^{2+}, the rate constant of Rod^{S}_{S} was 25% lower than that of Rod^{SH}_{SH}. Although the divalent metal ion clearly shows the expected effect, the observed change at neutral pH is relatively small [see also Reisler et al. (1983)].

(C) Kinetics of Formation of High Molecular Weight Species. A more detailed analysis for cross-linking the rod segment of myosin in myofibrils is presented in Figure 3, where the intensities of various oxidized rod species are plotted vs. cross-linking time. $(Rod^{S}_{S})_1$ decreased with time in a first-order decay process and was accompanied by an increase in rod dimers, $(Rod^{S}_{S})_2$, rod trimers, $(Rod^{S}_{S})_3$, and other rod species (M_r > 1000K; data not presented). It will be noted that the cross-linking kinetics of oxidized rod species, $(Rod^{S}_{S})_i$, follow a sequential reaction process; i.e., each rod species, $(Rod^{S}_{S})_i$, where $i \geq 2$, showed a biphasic profile whose decay was ac-

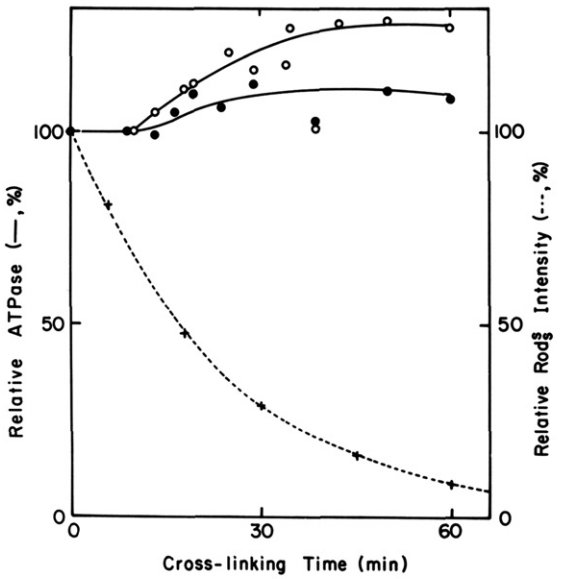

FIGURE 4: ATPase of myofibrils cross-linked by dimethyl suberimidate. Myofibrils were cross-linked as shown in Figure 1, and their relative ATPase was plotted vs. cross-linking time. (○) Actin-activated MgATPase; (●) CaATPase; (+) M_r 260K rod band (Rod_S^S) intensity.

companied by formation of higher molecular weight aggregates. Dotted lines (n = 2–4) in Figure 3 show the intensities of formation of higher molecular weight rod species; $\sum_{i=n}^{\infty}(Rod_S^S)_i$ where $n \geq 2$. The concentrations of the higher order species were calculated by assuming $\sum_{i=n}^{\infty}(Rod_S^S)_i = 100 - \sum_{i=1}^{n-1}(Rod_S^S)_i$ (%). As n becomes larger, a distinct lag in time in the appearance of high molecular weight rod species was observed despite the fact that the myosin heavy chain (MHC_{SH}^{SH}) as well as the Rod_S^S species followed first-order decay processes.

Relative Rates of Cross-Linking HMM and LMM Segments. Myofibrils were cross-linked with DMS (under the ionic conditions used in Figure 1A at 5, 15, and 25 °C, and cross-linked products were digested by chymotrypsin at various stages of the reaction at pH 8 (μ = 0.5 M), in the presence of 0.1 mM $CaCl_2$, to generate HMM and LMM segments. The intensity of each cross-linked myosin segment was determined by SDS gel electrophoresis, and the cross-linking rates were compared. We found that both HMM and LMM segments contribute to the cross-linking of the myosin heavy chains. The relative cross-linking time courses for these myosin segments showed similar profiles at each temperature although the absolute cross-linking rates were enhanced on elevating the temperature. However, the peptide band pattern on SDS gels was complex and precluded a detailed analysis of the cross-linking process (data not shown).

Effect of Cross-Linking on Myofibrillar ATPase. Since the effect of cross-linking on the contractile force of a muscle fiber will be examined in the following section, it was important to establish the effect of cross-linking on the biochemical process (ATP cleavage reaction) of muscle contraction. Myofibrils were cross-linked by DMS, and the specific ATP cleavage rates of cross-linked preparations were compared at various stages of reaction (Figure 4). Actin-activated MgATPase (open circles) as well as CaATPase (closed circles) showed a distinct and reproducible elevation in activity after 10-min cross-linking time. Although this effect could reflect some type of chemical modification within the ATP hydrolysis site of the S-1 subunit, it seems more likely that morphological changes in myofibrillar structure may be responsible for the apparent increase in ATPase. Light microscopic observations of myofibrils following activation showed that myofibrils were

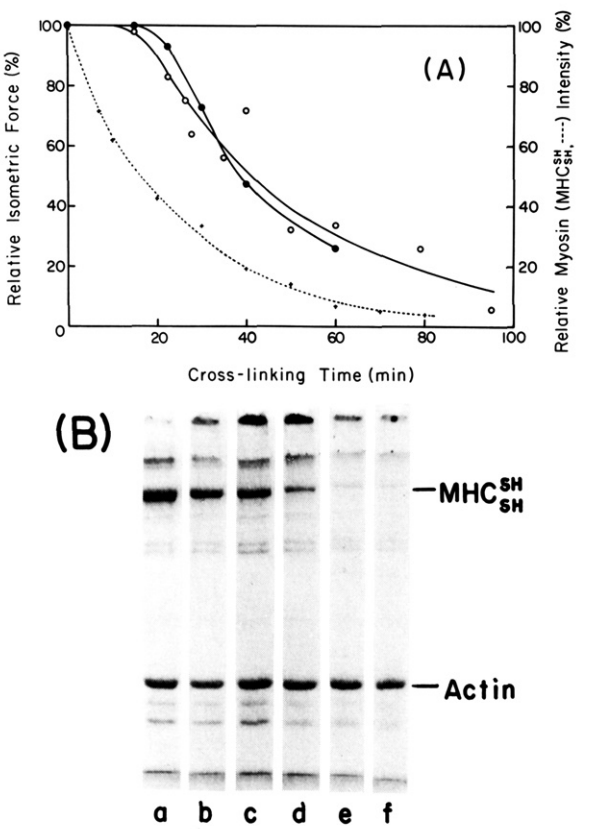

FIGURE 5: Effect of chemical cross-linking on isometric force in glycerinated fibers. (A) Glycerinated fibers dissected from rabbit psoas muscle were cross-linked with dimethyl suberimidate (2.0 mg/mL) at 10 °C in 40 mM cacodylate and 80 mM NaCl, pH 7.2 (open circles), or in 40 mM cacodylate, 20 mM NaCl, and 20 mM $MgCl_2$, pH 7.2 (closed circles), and relative isometric forces (f/f_0) developed in ATP-containing solution (see Materials and Methods) are plotted vs. cross-linking time. (B) Glycerinated fibers at various times of cross-linking were dissolved in 1% (w/v) SDS, 0.12 M Tris·HCl (pH 6.8), 10% (v/v) glycerol, 0.1% (v/v) 2-mercaptoethanol, and a trace of bromophenol blue and run on minislab gels employing 5% stacking and 8% separation gels according to Laemmli (1970). Cross-linking times (in minutes): (a) 0; (b), 7; (c) 20; (d) 40; (e) 60; (f) 80. The dotted line in (A) shows the myosin heavy-chain (MHC_{SH}^{SH}) intensity (normalized to the actin band intensity) vs. time plot.

contracted and condensed into globular structures at early stages of cross-linking but were more elongated at later stages (after-10 min cross-linking). It was also observed that myofibrillar MgATPase in the presence of EGTA (relaxed state) was about 5% of the active MgATPase, irrespective of the stage of cross-linking. The sustained high value of the ATP cleavage reaction seen in Figure 4, despite high levels of cross-linking, is in agreement with the findings of Baker and Cooke (1986) on the ATPase of cross-linked single fibers.

These observations, together with the finding that the S-1 subunits can be dissociated from actin in the presence of MgATP independent of the cross-linking reaction (see Figure 1C), provide evidence that chemical cross-linking with DMS does not substantially affect the normal actomyosin ATP hydrolysis cycle.

Effect of Cross-Linking on Isometric Force within Single Fibers. To investigate the effect of chemical cross-linking on the mechanical process of muscle contraction, glycerinated psoas fibers were cross-linked by DMS, and the relative isometric force (f/f_0) was determined at various cross-linking times. Cross-linking was carried out in the presence and absence of 20 mM Mg^{2+}. In both solvent systems, we observed a distinct lag time of about 20 min, where the force remained

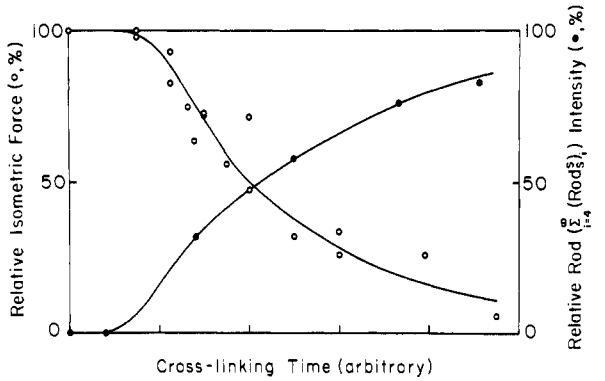

FIGURE 6: Correlation between isometric force and chemical cross-linking within myosin filament backbone. Figure 3 and 5 are summarized. Isometric force (as shown in Figure 5) and the intensity of high molecular weight cross-linked rod species (Figure 3, dotted line 4) are plotted vs. cross-linking time. The scale in time is arbitrary. MHC_{SH}^{SH} vs. time curves in Figures 3 and 5 were superimposed, and the force and the rod intensity data were expressed relative to the MHC_{SH}^{SH} intensity. (○) Isometric force. (●) High molecular weight rod species [$\sum_{i=4}^{\infty}(Rod_S^S)_i$] intensity.

unchanged (Figure 5A). This stage of the cross-linking reaction was followed by a monotonic decrease in isometric force. In these experiments, the time course of cross-linking within the thick filaments was determined by transferring single fibers at various stages of the reaction into SDS-containing solutions followed by SDS gel electrophoresis of the sample. The time dependence of the myosin heavy chain intensity (dotted line, Figure 5A) normalized to the actin band intensity was used as an internal control to compare the extent of cross-linking within a single fiber to that in the myofibrillar system.

Discussion

The present study provides evidence for a very low rate of (DMS) cross-linking of the S-1 subunits to rod segments of myosin within the thick filaments of myofibrils. Virtually no cross-linking of S-1 was detected under the environmental conditions employed for our experiments. This result suggests either that the surface area of S-1 in contact with rod segments of neighboring molecules is small or, alternatively, that the surface density of lysine residues near the S-1/rod interface is insufficient to allow rapid cross-linking. Despite the fact that S-1 is not cros-linked to rod segments or to actin (see below), intramolecular cross-linking reactions within the myosin head appear to be occurring, since the apparent molecular weight values of S-1-containing peptides increased from 90K to 90–120K during the cross-linking process (see Figure 1). Various factors such as chemical (monofunctional) modifications within S-1, intramolecular cross-linking within S-1 itself, and cross-linking between the S-1 heavy chain and its constituent light chain(s) may affect the mobilities of the S-1-containing peptides on SDS gels. In fact, Labbé et al. (1982) have reported that the heavy chain and light chain(s) of the S-1 subunit can be readily cross-linked.

The cross-linking of a glycerinated single fiber is accompanied by a loss in isometric force with little effect on the chemical (ATPase) process within myofibrils. Although it can be argued that the drop in force results from cross-linking of S-1 subunits to thin filaments, earlier work (Sutoh & Harrington, 1977) has shown that the rate of cross-linking rigor myosin heads to actin by DMS is not significant under the present cross-linking conditions. Kimura and Tawada (1984) reported similar conclusions based on DMS cross-linking of HMM–actin–tropomyosin complexes. Additionally, we observed no measurable change in the intensity of the actin band in the present study (Figure 1B) which could be attributed to this process. Although we cannot categorically exclude the formation of a small number of S-1/actin links, it seems to us unlikely that this putative intermolecular reaction could lead to the catastrophic fall in contractile force observed in Figure 5. Another possibility is that intramolecular cross-linking within the S-1 subunit, e.g., 120K S-1, is responsible for the decline in isometric force. However, this process appears to be pseudo first order (Figure 1D) whereas the present study and that of Baker and Cooke (1986) show a distinct lag phase in the isometric force vs. cross-linking time profile (Figure 5) suggesting that some type of cooperative interaction between adjoining elements within the thick filament core may be responsible for this behavior. Indeed, when the relative isometric force and the intensity of cross-linked species ($M_r \geq 1000K$) are plotted vs. MHC_{SH}^{SH}, we find that more than 50% of the myosin heavy-chain MHC_{SH}^{SH} is cross-linked intermolecularly and intramolecularly before the isometric force begins to decline. The relationship between the isometric force and the level of cross-linked rod species is shown in Figure 6, where the results in Figure 3 (dotted line, $n = 4$) and Figure 5A are combined relative to MHC_{SH}^{SH} and plotted vs. cross-linking time (using an arbitrary time scale). It will be seen that the isometric force vs. cross-linking time decreases in parallel with the formation of higher order cross-linked rod species ($\geq M_r$ 1000K). The relative force is compared with the cross-linked rod species, $\sum_{i=n}^{\infty}(Rod_S^S)_i$ where $n = 4$, in Figure 6, but this does not necessarily rule out other possibilities, such as $n = 3$, 5, 6, etc. The point we want to emphasize in these plots is that a sigmoidal drop in isometric force vs. cross-linking time appears to correlate with the intermolecular cross-linking profile of the rod species, despite the finding that MHC_{SH}^{SH} as well as Rod_{SH}^{SH} vs. time plots exhibit single-exponential decay processes.

Although an unambiguous interpretation of the relative chemical cross-linking of HMM and LMM segments was difficult in this study, it is worth noting that the chymotryptic cleavage of cross-linked myofibrils to release HMM and LMM segments showed two distinct stages. The log (relative intensity of HMM or LMM) vs. cross-linking time plot showed a shallow first-order slope at an early stage and then sharply declined at a later stage in contrast to the time course of cross-linking rod and S-1 segments. This sharp drop in the late stages of the reaction corresponded to the catastrophic drop in force, suggesting that chemical cross-linking within the thick filament backbone affects force production.

It is striking that the mobile myosin heads appear to cycle through neighboring actin filaments, cleaving ATP at an undiminished rate, as the isometric force declines and the thick filament core undergoes extensive cross-linking. Thus, our results focus on the importance of the core region of the thick filament in the force-generating process and suggest that release of the S-2 element from the filament surface in the bridge cycle is an essential component of this process.

Acknowledgments

We are indebted to Drs. Anthony Baker and Roger Cooke for their helpful comments and for sending us details of their cross-linking experiments on psoas fibers prior to publication. We are also grateful to Dr. Michael Rodgers, Stephen Lovell, and Julien Davis for very useful discussions.

Registry No. Mg, 7439-95-4.

References

Baker, A. J., & Cooke, R. (1986) *Biophys. J. 49*, 7a.

Borejdo, J., & Weber, M. M. (1982) *Biochemistry 21*, 549–555.

Brenner, B. (1983) *Biophys. J. 41*, 99-102.
Chiao, Y. C., & Harrington, W. F. (1979) *Biochemistry 18*, 959-963.
Harrington, W. F. (1971) *Proc. Natl. Acad. Sci. U.S.A. 68*, 685-689.
Harrington, W. F. (1979) *Proc. Natl. Acad. Sci. U.S.A. 76*, 5066-5070.
Kimura, M., & Tawada, K. (1984) *Biophys. J. 45*, 603-610.
Kundrat, E., & Pepe, F. A. (1971) *J. Cell Biol. 48*, 340-347.
Labbé, J. P., Mornet, D., Roseau, G., & Kassab, R. (1982) *Biochemistry 21*, 6897-6902.
Laemmli, U. K. (1970) *Nature (London) 227*, 680-685.
Peacock, A. C., & Dingman, C. W. (1968) *Biochemistry 7*, 668-674.
Persechini, A., & Rowe, A. J. (1984) *J. Mol. Biol. 172*, 23-39.
Piper, J. M., & Lovell, S. J. (1981) *Anal. Biochem. 117*, 70-75.
Reisler, E., Liu, J., & Cheung, P. (1983) *Biochemistry 22*, 4954-4960.
Rodgers, M. E. (1982) Ph.D. Thesis, The Johns Hopkins University.
Rome, E. (1967) *J. Mol. Biol. 27*, 591-602.
Sutoh, K., & Harrington, W. F. (1977) *Biochemistry 16*, 2441-2449.
Sutoh, K., Chiao, Y. C., & Harrington, W. F. (1978) *Biochemistry 17*, 1234-1239.
Ueno, H., & Harrington, W. F. (1981) *J. Mol. Biol. 149*, 619-640.
Ueno, H., & Harrington, W. F. (1986) *J. Mol. Biol. 190*, 57-68.
Ueno, H., Rodgers, M., & Harrington, W. F. (1983) *J. Mol. Biol. 186*, 207-228.
Weeds, A. G., & Pope, B. (1977) *J. Mol. Biol. 111*, 129-157.

Control of Placental Alkaline Phosphatase Gene Expression in HeLa Cells: Induction of Synthesis by Prednisolone and Sodium Butyrate

Janice Yang Chou* and Shori Takahashi

Human Genetics Branch, National Institute of Child Health and Human Development, National Institutes of Health, Bethesda, Maryland 20892

Received October 29, 1986; Revised Manuscript Received January 15, 1987

ABSTRACT: HeLa S_3 cells produce an alkaline phosphatase indistinguishable from the enzyme from human term placenta. The phosphatase activity in these cells was induced by both prednisolone and sodium butyrate. Both agents stimulated de novo synthesis of the enzyme. The increase in phosphatase activity paralleled the increase in immunoactivity and biosynthesis of placental alkaline phosphatase. The fully processed phosphatase monomer in control, prednisolone-treated or butyrate-treated cells was a 64.5K polypeptide, measured by both incorporation of L-[^{35}S]methionine into enzyme protein and active-site labeling. The 64.5K polypeptide was formed by the incorporation of additional *N*-acetylneuraminic acid moieties to a precursor polypeptide of 61.5K. However, this biosynthetic pathway was identified only in butyrate-treated cells. In prednisolone-treated cells, the processing of 61.5K to the 64.5K monomer was accelerated, and the presence of the 61.5K precursor could only be detected by either neuraminidase or monensin treatment. Phosphatase mRNA which comigrated with the term placental alkaline phosphatase mRNA of 2.7 kilobases was induced in the presence of either prednisolone or butyrate. Alkaline phosphatase mRNA in untreated HeLa S_3 cells migrated slightly faster than the term placental alkaline phosphatase mRNA. Butyrate also induced a second still faster migrating alkaline phosphatase mRNA. Both prednisolone and butyrate increased the steady-state levels of placental alkaline phosphatase mRNA. Our data indicate that the increase in phosphatase mRNA by prednisolone and butyrate resulted in the induction of alkaline phosphatase activity and biosynthesis in HeLa S_3 cells. Furthermore, both agents induced the expression of different alkaline phosphatase gene transcripts without altering its protein product.

Human term placental alkaline phosphatase (orthophosphoric-monoester phosphohydrolase; alkaline pH; EC 3.1.3.1) is a membrane-bound tissue-specific glycoprotein (Badger & Sussman, 1976; Mulivor et al., 1978a). In addition to the gene locus encoding term placental alkaline phosphatase, there exist at least two other gene loci encoding human alkaline phosphatases. They are the gene locus encoding adult intestinal alkaline phosphatase and the gene locus encoding tissue-unspecific alkaline phosphatase which is the major isozyme expressed in liver, kidney, and bone (Sussman et al., 1968; Gottlieb & Sussman, 1968; Mulivor et al., 1978a,b). A great deal of interest in the term placental alkaline phosphatase has stemmed from the finding that this enzyme was produced ectopically by a lung cancer (Fishman et al., 1968). It was subsequently found that term placental alkaline phosphatase or term placental alkaline phosphatase like enzyme was produced by a variety of trophoblastic and nontrophoblastic tumors and tumor-derived cell lines [for reviews, see Fishman and Stolbach (1979) and Stigbrand et al. (1982)]. Thus, an understanding of the mechanism which controls the expression of term placental alkaline phosphatase gene is likely to yield insight into the transformation process.

Alkaline phosphatase activity in cultured placental and nonplacental cells can be modulated by a variety of hormones and agents (Ghosh et al., 1972; Bulmer et al., 1976; Hamilton et al., 1979; Hanford et al., 1981; Mulkins et al., 1983; Ito

* Correspondence should be addressed to this author.